Electronic Supplementary Material (ESI) for Organic & Biomolecular Chemistry.

Supporting Information

Binding-Promoted Chemical Reaction in the Nanospace of a Binding Site: Effects of Environmental Constriction

Xiaoyu Xing and Yan Zhao*

Department of Chemistry, Iowa State University, Ames, Iowa 50011-3111, USA

Table of Contents

General Method

All other reagents and solvents were of ACS-certified grade or higher, and were used as received from commercial suppliers. Routine ^{1}H and ^{13}C NMR spectra were recorded on a Bruker DRX-400, on a Bruker AV II 600 or on a Varian VXR-400 spectrometer. ESI-MS mass was recorded on Shimadzu LCMS-2010 mass spectrometer. Dynamic light scattering (DLS) data were recorded at 25 °C using PDDLS/ CoolBatch 90T with PD2000DLS instrument. Fluorescence spectra were recorded at ambient temperature on a Varian Cary Eclipse Fluorescence spectrophotometer.

Scheme S1

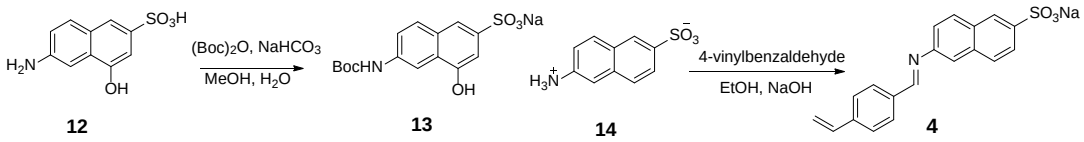

12 **13** **14** **4**

Scheme S2

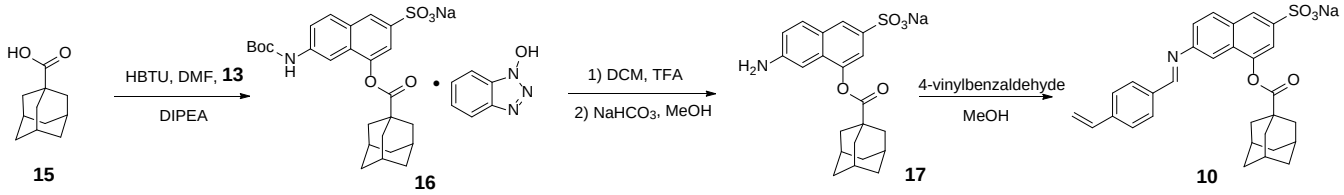

15 **16** **17** **10**

Syntheses

4-vinylbenzaldehyde was synthesized following reported procedures.[1]

Compound 13. 6-Amino-4-hydroxy-2-naphthalenesulfonic acid (500 mg, 2.09 mmol), di-t-butyl dicarbonate (912 mg, 4.18 mmol), and sodium bicarbonate (351 mg, 4.18 mmol) were dissolved in a mixture of 50 mL of methanol and 2 mL of water. The reaction mixture was heated to 60 °C and stirred overnight. After the reaction mixture was concentrated by rotary evaporation, the residue was purified by flash column chromatography over silica gel with 15:1 ethyl acetate/methanol as the eluent to give a

[1] D. Song, S. Cho, Y. Han, Y. You, W. Nam, *Org. Lett.* **2013**, *15*, 3582-3585.

pink powder (539 mg, 71%). ^{1}H NMR (400 MHz, CD_3OD, δ) 8.29 (d, *J* = 2.2 Hz, 1H), 7.80 – 7.74 (m, 2H), 7.55 (dd, *J* = 8.9, 2.2 Hz, 1H), 7.22 (d, *J* = 1.5 Hz, 1H), 1.55 (s, 9H). ^{13}C NMR (151 MHz, CD_3OD, δ) 154.0, 152.8, 140.4, 137.3, 129.9, 128.74, 126.4, 120.2, 116.1, 109.3, 104.8, 79.7, 27.4. ESI-MS (*m/z*): $[M\text{-}Na]^-$ cacld for $C_{15}H_{16}NO_6S$, 338.0704; found, 338.0706.

Compound 16. Compound **13** (27.4 mg, 0.152 mmol), HBTU (105 mg, 0.277 mmol), and DIPEA (89 mg, 0.689 mmol) were dissolved in 5 mL of DMF. After the reaction mixture as stirred for 30 min, compound **15** (50 mg, 0.138 mmol) was added. The reaction mixture was stirred at room temperature overnight. After the mixture was concentrated by rotary evaporation, the residue was purified by flash column chromatography over silica gel with 20:1 dichloromethane/methanol as the eluent to give a light-yellow powder (61.1 mg, 61%). ^{1}H NMR (400 MHz, CD_3OD, δ) 8.18 (s, 1H), 8.15 (s, 1H), 7.89 – 7.86 (m, 2H), 7.74 (d, *J* = 8.5 Hz, 1H), 7.56 – 7.44 (m, 4H), 2.26 (d, *J* = 2.9 Hz, 6H), 2.14 (s, 3H), 1.89 (s, 6H), 1.55 (s, 9H). ^{13}C NMR (151 MHz, CD_3OD, δ) 177.53, 154.82, 147.72, 141.30, 140.57, 130.93, 130.65, 129.69, 127.95, 127.04, 124.00, 121.71, 118.51, 116.96, 111.59, 108.52, 81.03, 48.43, 42.58, 40.05, 37.52, 29.48, 28.65, 19.26. ESI-MS (*m/z*): $[M\text{-}HOBt\text{-}Na]^-$ cacld for $C_{26}H_{30}NO_7S$, 500.1743; found, 500.1759.

Compound 17. Compound **16** (61.1 mg, 0.093 mmol) was dissolved in 10 mL of trifluoroacetic acid. The reaction mixture was stirred at room temperature overnight. After the reaction mixture was concentrated by rotary evaporation, the residue was re-dissolved in 25 mL methanol with sodium bicarbonate (23.4 mg, 0.279 mmol). After stirred for 30 min, the reaction mixture was concentrated by rotary evaporation and the residue was purified by flash column chromatography over silica gel with 15:1 dichloromethane/methanol as the eluent to give a white powder (30.3 mg, 77%). ^{1}H NMR (400 MHz, CD_3OD, δ) 8.03 (s, 1H), 7.72 (d, *J* = 8.8 Hz, 1H), 7.39 (d, *J* = 1.6 Hz, 1H), 7.07 (dd, *J* = 8.8, 2.2 Hz, 1H), 6.86 (d, *J* = 2.2 Hz, 1H), 2.22 (d, *J* = 2.9 Hz, 6H), 2.14 (s, 3H), 1.87 (t, *J* = 3.2 Hz, 6H). ^{13}C NMR (151 MHz, CD_3OD, δ) 177.81, 149.60, 146.20, 131.16, 130.92, 128.52, 124.41, 120.91, 116.60, 101.60, 42.59, 40.12, 37.49, 29.43. ESI-MS (*m/z*): $[M\text{-}Na]^-$ cacld for $C_{21}H_{22}NO_5S$, 400.1219; found, 400.1218.

Compound 4. Compound **14** (0.020 mmol, 4.5 mg), 4-vinylbenzaldehyde (13.2 mg, 0.100 mmol), and sodium hydroxide (0.020 mmol, 0.8 mg) were mixed with 10 mL of ethanol. The reaction mixture was heated to reflux overnight and cooled to room temperature. Diethyl ether (40 mL) was added slowly. The precipitate formed was collected by filtration and washed with 5 mL of diethyl ether to yield a yellow powder (5.7 mg, 79.3%). The product was used in the MINP preparation without further purification. ^{1}H NMR (500 MHz, DMSO-d_6, δ) 8.78 (s, 1H), 8.17 (s, 1H), 8.03 (d, *J* = 8.7 Hz, 1H), 7.97 (d, *J* = 7.8 Hz,

2H), 7.89 (d, *J* = 8.6 Hz, 1H), 7.73 (d, *J* = 5.4 Hz, 2H), 7.65 (d, *J* = 7.8 Hz, 2H), 7.54 (dd, *J* = 8.4, 2.2 Hz, 1H), 6.83 (dd, *J* = 17.6, 11.0 Hz, 1H), 5.99 (d, *J* = 17.7 Hz, 1H), 5.40 (d, *J* = 10.9 Hz, 1H).

Compound 10. Compound **17** (0.020 mmol, 8.5 mg) and 4-vinylbenzaldehyde (13.2 mg, 0.100 mmol) were mixed with 10 mL of methanol. The reaction mixture was stirred overnight. Diethyl ether (40 mL) was added slowly. The precipitate formed was collected by filtration and washed with 5 mL of diethyl ether to yield a brown powder (9.8 mg, 85.4%). The product was used in the MINP preparation without further purification. ^{1}H NMR (400 MHz, DMSO-d_6, δ) 8.75 (s, 1H), 8.13 (d, *J* = 8.7 Hz, 1H), 8.09 (s, 1H), 7.97 (d, *J* = 7.1 Hz, 2H), 7.66 (d, *J* = 7.8 Hz, 2H), 7.60 (d, *J* = 8.8 Hz, 1H), 7.42 (s, 1H), 7.37 (s, 1H), 6.83 (dd, *J* = 17.6, 11.0 Hz, 1H), 6.00 (d, *J* = 17.8 Hz, 1H), 5.41 (d, *J* = 10.9 Hz, 1H), 2.09-2.15 (m, 9H), 1.74-1.81 (m, 6H).

Preparation of MINPs.

MINPs were synthesized according to previously reported procedures.[2] To a micellar solution of **1** (10.2 mg, 0.02 mmol) in H_2O (2.0 mL), divinylbenzene (DVB, 2.8 μL, 0.02 mmol), the template–FM complex (**4** or **10**) in DMSO (0.0004 mmol), and 2,2-dimethoxy-2-phenylacetophenone (DMPA) in DMSO (10 μL of a 12.8 mg/mL, 0.0005 mmol) were added. The mixture was sonicated for 10 min. Cross-linker **2** (4.1 mg, 0.024 mmol), $CuCl_2$ in H_2O (10 μL of 6.7 mg/mL, 0.0005 mmol), and sodium ascorbate in H_2O (10 μL of 99 mg/mL, 0.005 mmol) were then added and the reaction mixture was stirred slowly at room temperature for 12 h. Compound **3** (10.6 mg, 0.04 mmol), $CuCl_2$ (10 μL of a 6.7 mg/mL solution in H_2O, 0.0005 mmol), and sodium ascorbate (10 μL of a 99 mg/mL solution in H_2O, 0.005 mmol) were then added and the solution stirred for another 6 h at room temperature. The reaction mixture was transferred to a glass vial, purged with nitrogen for 15 min, sealed with a rubber stopper, and irradiated in a Rayonet reactor for 12 h. The reaction mixture was poured into acetone (8 mL). The precipitate was collected by centrifugation and washed with a mixture of methanol/acetic acid (5 mL/0.1 mL) three times. The off-white product was dried in air to afford the final MINPs (> 80%).

Preparation of MINP-CHO.

$MINP_4$ (15.2 mg) was sonicated in 2 mL of 6 M hydrochloric acid for 20 min. The resulting solution was stirred at 95 °C for 2 h and then was poured into acetone (8 mL). The precipitate formed was collected by

[2] Arifuzzaman, M. D.; Zhao, Y. *J. Org. Chem.* **2017**, *81*, 7518.

centrifugation and washed with a mixture of acetone/water (5 mL/1 mL) three times. The off-white product was dried in air to afford the MINP$_4$-CHO (12.0 mg, 79%).

Preparation of MINP$_4$-CH$_2$OH.

MINP$_4$-CHO (12.0 mg) were sonicated in 1 mL of anhydrous DMF for 20 min until fully dissolved. An aliquot of sodium borohydride stock solution (37.9 mg in 1 mL of anhydrous DMF) was added to the MINP$_4$-CHO solution. After stirred overnight, the reaction mixture was poured into acetone (8 mL). The precipitate was collected by centrifugation and washed with a mixture of acetone/water (5 mL/1 mL) three times, and then a mixture of methanol/acetic acid (5 mL/0.1 mL) three times. The off-white product was dried in air. To remove the borate ions, the MINP$_4$-CH$_2$OH was re-dissolved and stirred with 2 mL of sodium chloride solution (5000 equiv based on MINP concentration) overnight. The solution was transferred to a dialysis tube (MWCO 3.5K). The tube was placed in 2 L of deionized water with gentle stirring. The dialysis tube was sonicated and the water was changed after 2, 4, 6, and 20 h. After 48 h, the MINP solution was poured into 40 mL of acetone and the precipitate was collected by centrifugation. The precipitate was dried in air to afford MINP$_4$-CH$_2$OH (8.6 mg, 72%).

Titration by Fluorescence Spectroscopy and Data Analysis Method

A stock solution of MINP-CHO (200 μM) was prepared in 10 mM HEPES buffer (pH 7) or DMF. Stock solutions (200 μM) of the guests (**5**-**9**) were prepared in water. For the titrations, a typical procedure is as follows. An aliquot of the guest stock solution was added to 2.00 mL of the appropriate solvent (HEPES buffer or DMF) in a quartz cuvette. The concentration of the guest was 0.5 μM. The sample was gently vortexed for 30 s before its fluorescence spectrum was recorded. Aliquots of the MINP solution was added and the spectrum was recorded after each addition. The titration was continued until saturation was reached and the total volume of the MINP solution added was kept below 100 μL. The binding constant was obtained by nonlinear least squares curving fitting of the emission intensity to the 1:1 binding isotherm.[3] All titrations were performed at room temperature unless indicated otherwise.

[3] Schneider, H. J.; Yatsimirsky, A. K. *Principles and methods in supramolecular chemistry*; New York: J. Wiley, 2000; pp 137-146.

Imine Formation Monitored by Fluorescence Spectroscopy

A stock solution of MINP-CHO and **11** (200 μM) was prepared in DMF. Stock solutions of the guests (**5-9**, 200 μM) were prepared in water. For the imine formation, a typical procedure is as follows. An aliquot of the amine stock solution was added to 2.00 mL of DMF in a quartz cuvette. The concentration of the amine was 0.5 μM. The sample was gently vortexed for 30 s and kept in a temperature-controlled cuvette holder for 5 min to reach the set temperature before its fluorescence spectrum was recorded. An aliquot of the MINP-CHO solution was added to the cuvette. The concentration of MINP-CHO was 5.0 μM. Fluorescence spectra were collected over time and the rate constant was obtained by nonlinear least squares curve fitting to the pseudo first-order rate law, in which F_t is the fluorescence intensity at time t, F_0 the initial intensity, and F_∞ the intensity at the completion of the reaction.

$$ln\frac{F_t - F_0}{F_0 - F_\infty} = -k_{obs}t$$

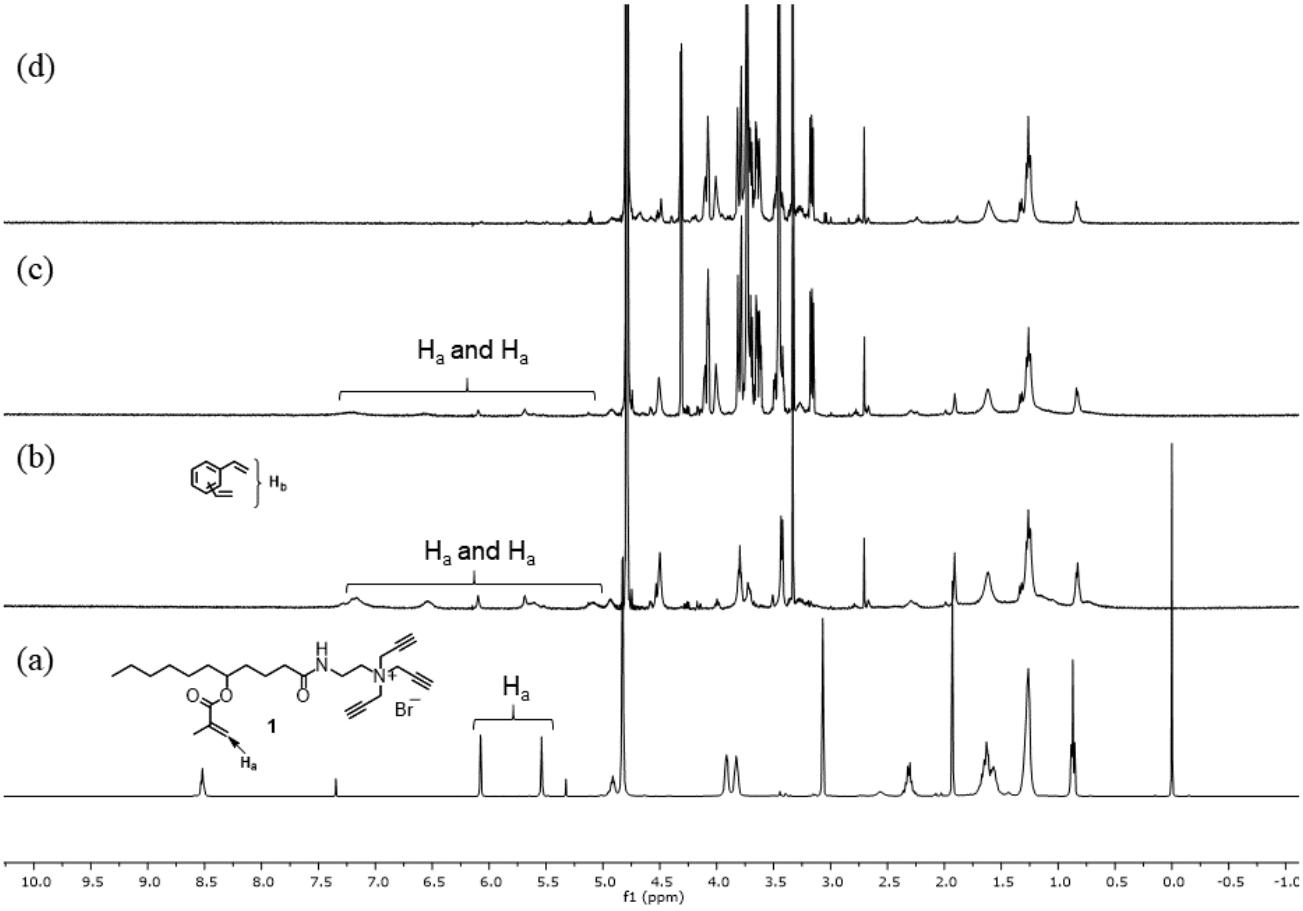

Figure S1. ^{1}H NMR spectra of (a) surfactant **1** in $CDCl_3$, (b) surface-cross-linked micelles (SCM) in D_2O, (c) surface-functionalized SCM in D_2O, and (d) core-cross-linked micelles in D_2O for MINP**4**.

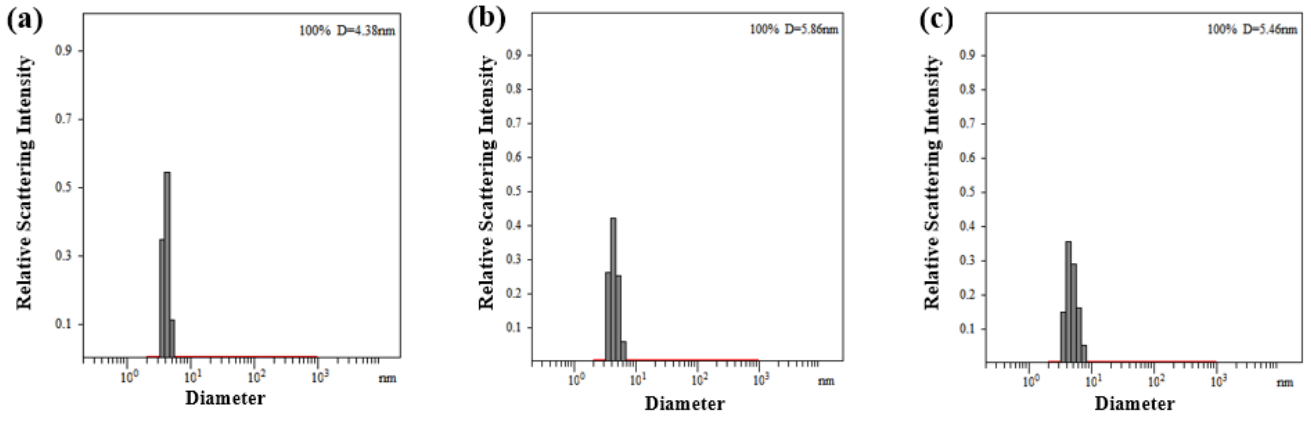

Figure S2. Distribution of the hydrodynamic diameters of the nanoparticles in water as determined by DLS for (a) surface-cross-linked micelles (SCM), (b) surface-functionalized SCM, and (c) purified $MINP_4$.

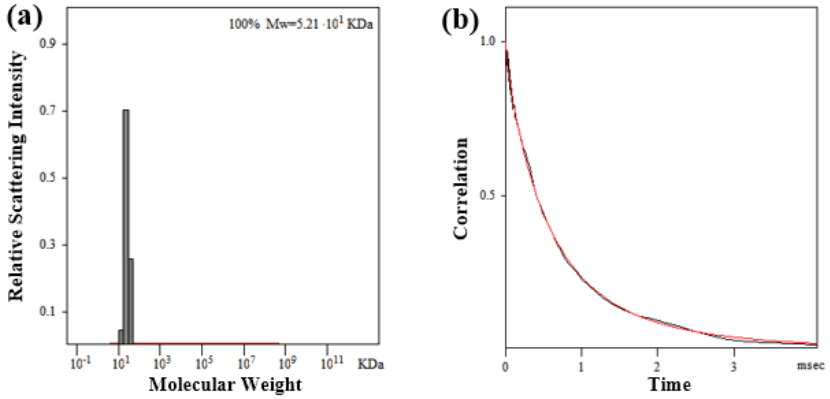

Figure S3. Distribution of the molecular weights and the correlation curve for $MINP_4$ from the DLS. The PRECISION DECONVOLVE program assumes the intensity of scattering is proportional to the mass of the particle squared. If each unit of building block for the MINP is assumed to contain one molecule of surfactant (MW = 465 g/mol), 1.2 molecules of cross linker (MW = 172 g/mol), one molecule of DVB (MW = 130 g/mol), and 0.8 molecules of sugar derivative (MW = 264 g/mol), the molecular weight of MINP translates to 51 [= 52100 / (465 + 1.2×172 + 130 + 0.8×264)] of such units.

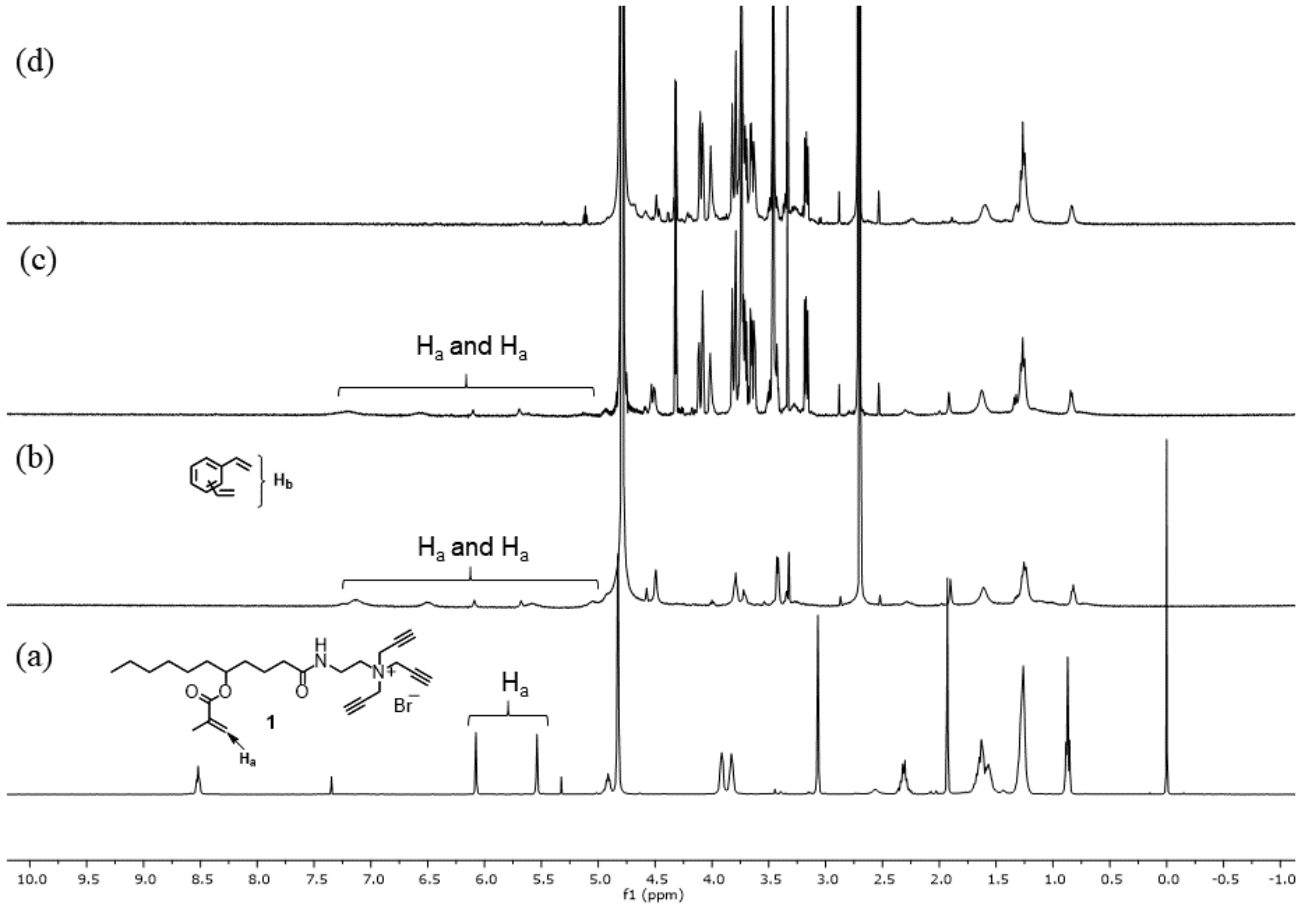

Figure S4. ^{1}H NMR spectra of (a) surfactant **1** in $CDCl_3$, (b) surface-cross-linked micelles (SCM) in D_2O, (c) surface-functionalized SCM in D_2O, and (d) core-cross-linked micelles in D_2O for $MINP_{\mathbf{10}}$.

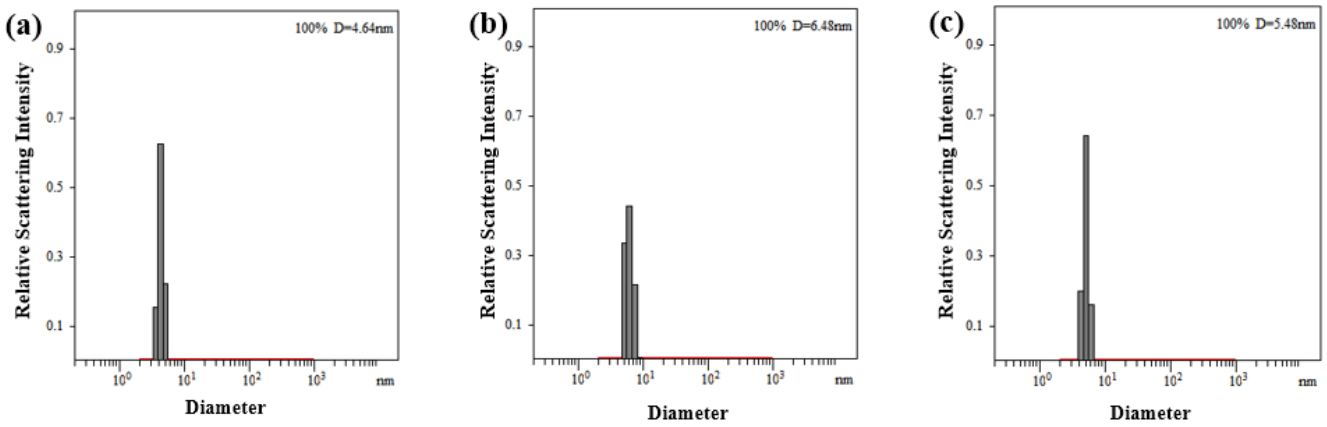

Figure S5. Distribution of the hydrodynamic diameters of the nanoparticles in water as determined by DLS for (a) surface-cross-linked micelles (SCM), (b) surface-functionalized SCM, and (c) purified $MINP_{10}$.

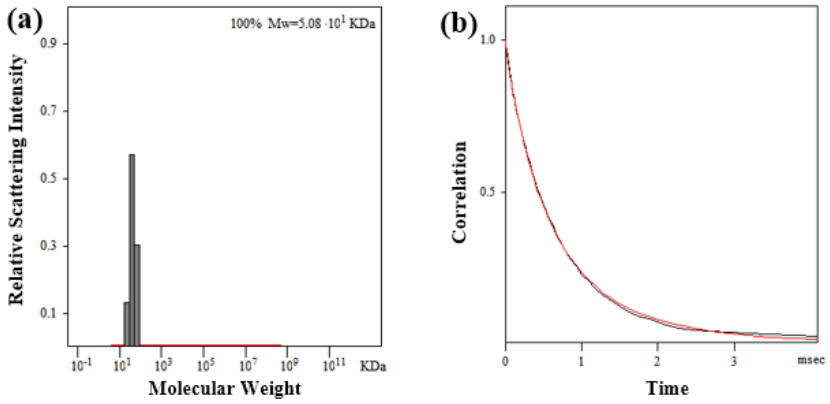

Figure S6. Distribution of the molecular weights and the correlation curve of $MINP_{10}$ from the DLS. The PRECISION DECONVOLVE program assumes the intensity of scattering is proportional to the mass of the particle squared. If each unit of building block for the MINP is assumed to contain one molecule of surfactant (MW = 465 g/mol), 1.2 molecules of cross linker (MW = 172 g/mol), one molecule of DVB (MW = 130 g/mol), and 0.8 molecules of sugar derivative (MW = 264 g/mol), the molecular weight of MINP translates to 50 [= 50800 / (465 + 1.2×172 + 130 + 0.8×264)] of such units.

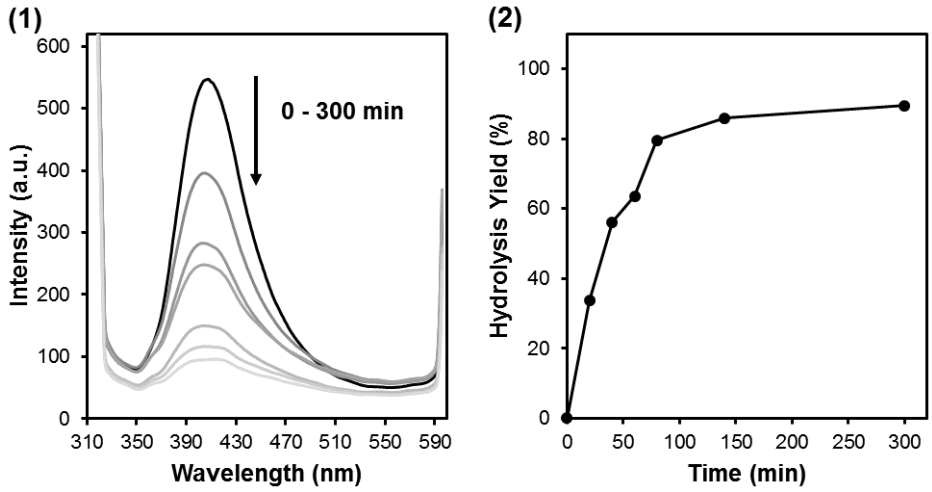

Figure S7. (1) Fluorescence spectra of MINP$_4$ during hydrolysis process. (2) Hydrolysis yield calculated based on fluorescence. To calculate the hydrolysis yield, an aliquot (40 μL) of the hydrolyzed reaction mixture was poured into acetone (10 mL). The precipitate was collected by centrifugation and washed three times with acetone (5 mL). After dried in air, the sample was dissolved in 2.00 mL of water with sonication. The fluorescence spectrum was then recorded. The hydrolysis yield was calculated based on the initial intensity.

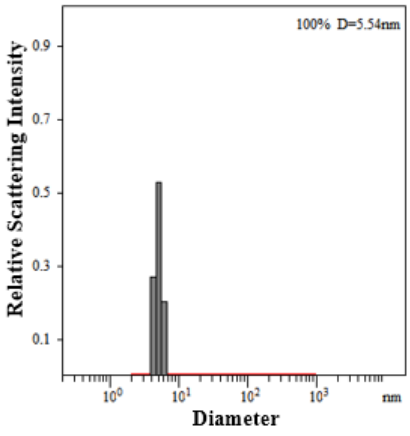

Figure S8. Distribution of the hydrodynamic diameters of the nanoparticles in water as determined by DLS for MINP$_4$ after HCl hydrolysis.

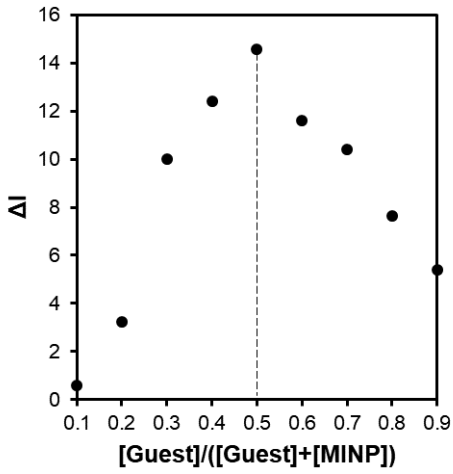

Figure S9. Job plot for $MINP_4$-CHO with **5** in DMF by fluorescence. The total concentration of MINP and the guest was 1.0 μM.

Fluorescence Titrations

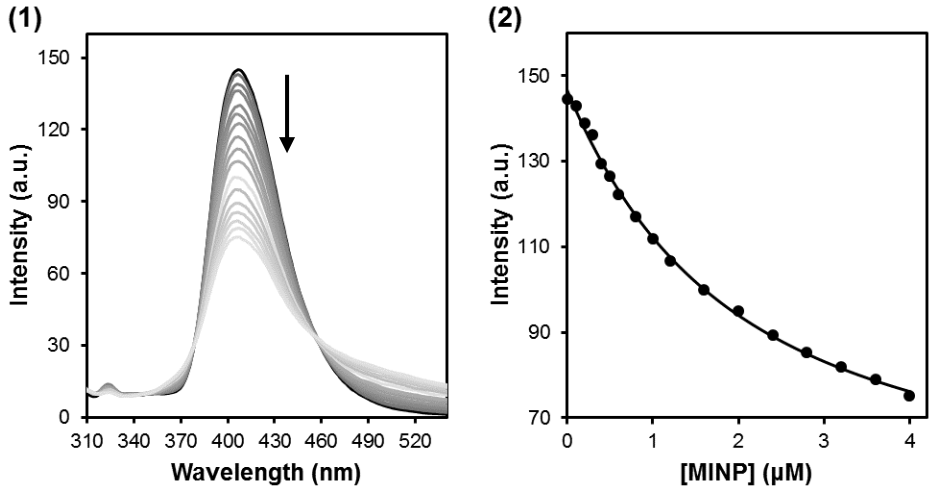

Figure S10. (1) Emission spectra of **5** upon the addition of different concentrations of MINP$_4$-CHO in DMF. [**5**] = 0.5 μM. The concentration of MINP was calculated based on an approximate M.W. of 50000 g/mol. λ_{ex} = 295 nm. (2) Plot of intensity at 406 nm with concentration of MINP and nonlinear least squares fitting of the emission intensity at 406 nm to a 1:1 binding isotherm. (Table 1, entry 1)

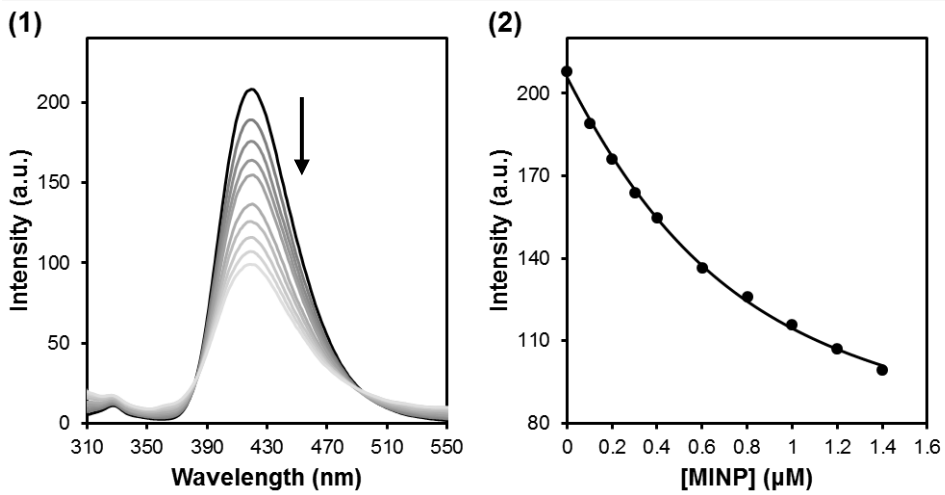

Figure S11. (1) Emission spectra of **5** upon the addition of different concentrations of MINP$_4$-CHO in 10 mM HEPES buffer pH 7.0. [**5**] = 0.5 μM. The concentration of MINP was calculated based on an approximate M.W. of 50000 g/mol. λ_{ex} = 295 nm. (2) Plot of intensity at 420 nm with concentration of MINP and nonlinear least squares fitting of the emission intensity at 420 nm to a 1:1 binding isotherm. (Table 1, entry 1 in parentheses)

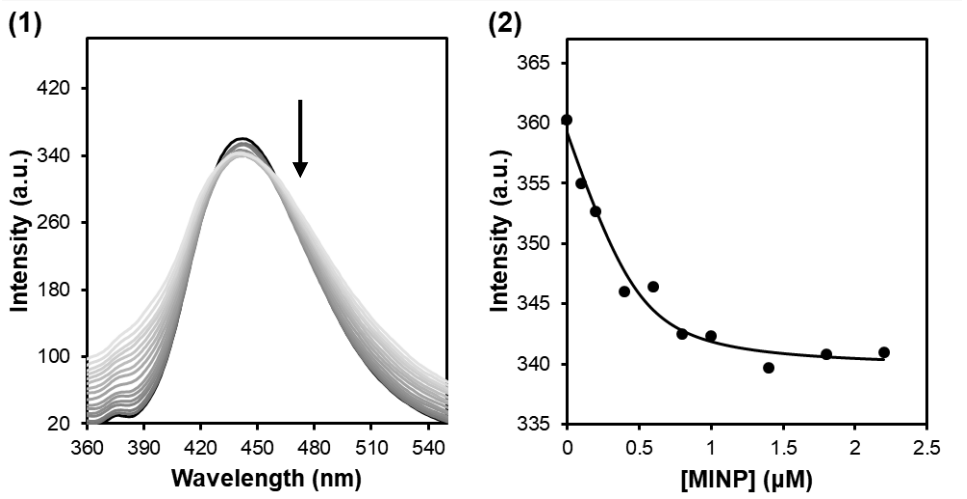

Figure S12. (1) Emission spectra of **6** upon the addition of different concentrations of MINP$_4$-CHO in DMF. [**6**] = 0.5 μM. The concentration of MINP was calculated based on an approximate M.W. of 50000 g/mol. λ_{ex} = 338 nm. (2) Plot of intensity at 440 nm with concentration of MINP and nonlinear least squares fitting of the emission intensity at 440 nm to a 1:1 binding isotherm. (Table 1, entry 2)

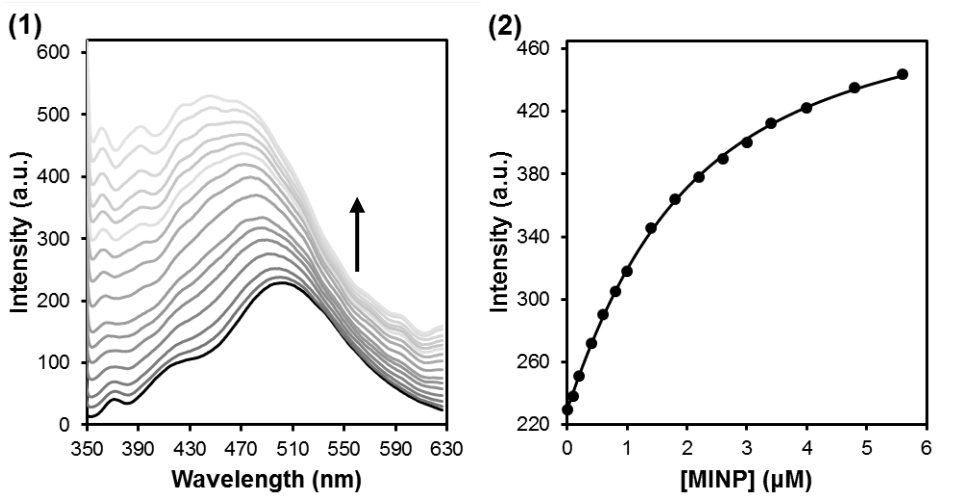

Figure S13. (1) Emission spectra of **6** upon the addition of different concentrations of MINP$_4$-CHO in 10 mM HEPES buffer pH 7.0. [**6**] = 1.0 μM. The concentration of MINP was calculated based on an approximate M.W. of 50000 g/mol. λ_{ex} = 330 nm. (2) Plot of intensity at 500 nm with concentration of MINP and nonlinear least squares fitting of the emission intensity at 500 nm to a 1:1 binding isotherm. (Table 1, entry 2 in parentheses)

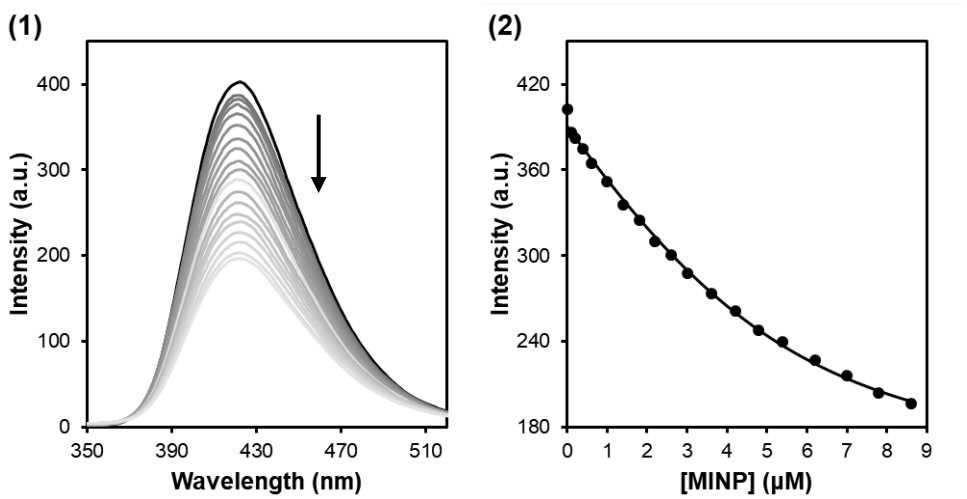

Figure S14. (1) Emission spectra of **7** upon the addition of different concentrations of MINP$_4$-CHO in DMF. [**7**] = 5.0 μM. The concentration of MINP was calculated based on an approximate M.W. of 50000 g/mol. λ_{ex} = 335 nm. (2) Plot of fluorescence intensity at 420 nm with concentration of MINP and nonlinear least squares fitting of the emission intensity at 420 nm to a 1:1 binding isotherm. (Table 1, entry 3)

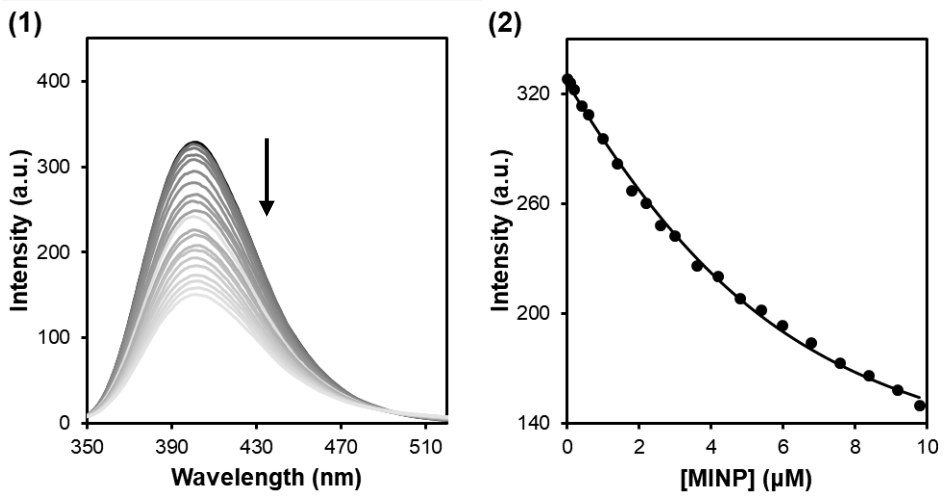

Figure S15. (1) Emission spectra of **8** upon the addition of different concentrations of MINP$_4$-CHO in DMF. [**8**] = 5.0 μM. The concentration of MINP was calculated based on an approximate M.W. of 50000 g/mol. λ_{ex} = 335 nm. (2) Plot of fluorescence intensity at 400 nm with concentration of MINP and nonlinear least squares fitting of the emission intensity at 400 nm to a 1:1 binding isotherm. (Table 1, entry 4)

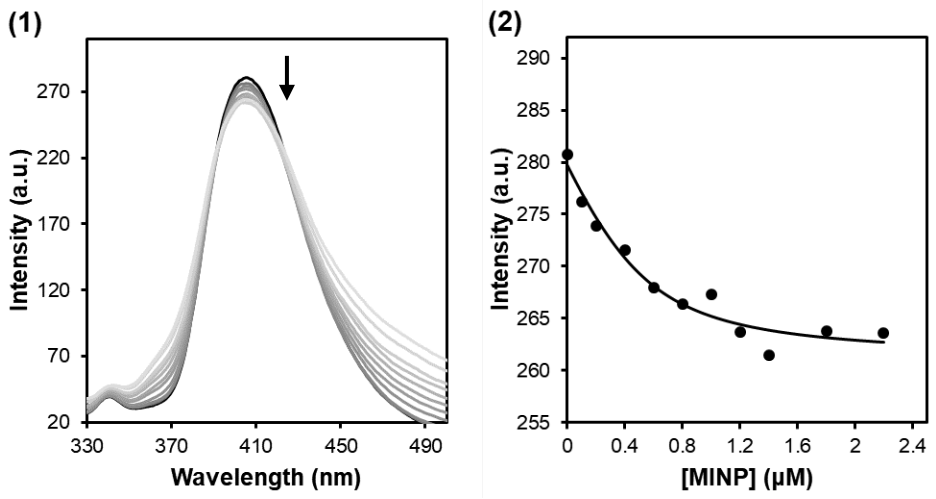

Figure S16. (1) Emission spectra of **9** upon the addition of different concentrations of MINP$_4$-CHO in DMF. [**9**] = 0.5 μM. The concentration of MINP was calculated based on an approximate M.W. of 50000 g/mol. λ_{ex} = 309 nm. (2) Plot of fluorescence intensity at 406 nm with concentration of MINP and nonlinear least squares fitting of the emission intensity at 406 nm to a 1:1 binding isotherm. (Table 1, entry 5)

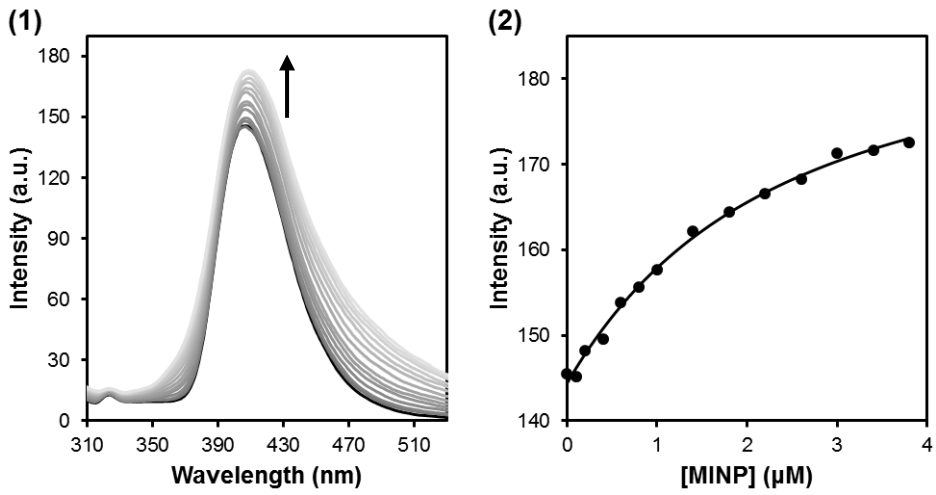

Figure S17. (1) Emission spectra of **5** upon the addition of different concentrations of MINP$_4$-CH_2OH (reduced by $NaBH_4$ from MINP$_4$-CHO) in DMF. [**5**] = 0.5 μM. The concentration of MINP was calculated based on an approximate M.W. of 50000 g/mol. λ_{ex} = 295 nm. (2) Plot of intensity at 406 nm with concentration of MINP and nonlinear least squares fitting of the emission intensity at 406 nm to a 1:1 binding isotherm. (Table 1, entry 6)

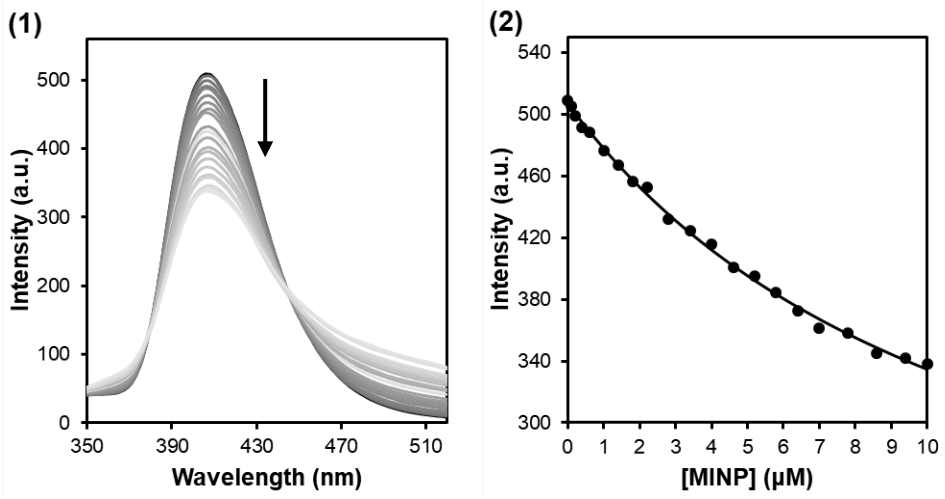

Figure S18. (1) Emission spectra of **5** upon the addition of different concentrations of $MINP_{10}$-CHO in DMF. [**5**] = 0.5 μM. The concentration of MINP was calculated based on an approximate M.W. of 50000 g/mol. λ_{ex} = 295 nm. (2) Plot of intensity at 406 nm with concentration of MINP and nonlinear least squares fitting of the emission intensity at 406 nm to a 1:1 binding isotherm. (Table 1, entry 7)

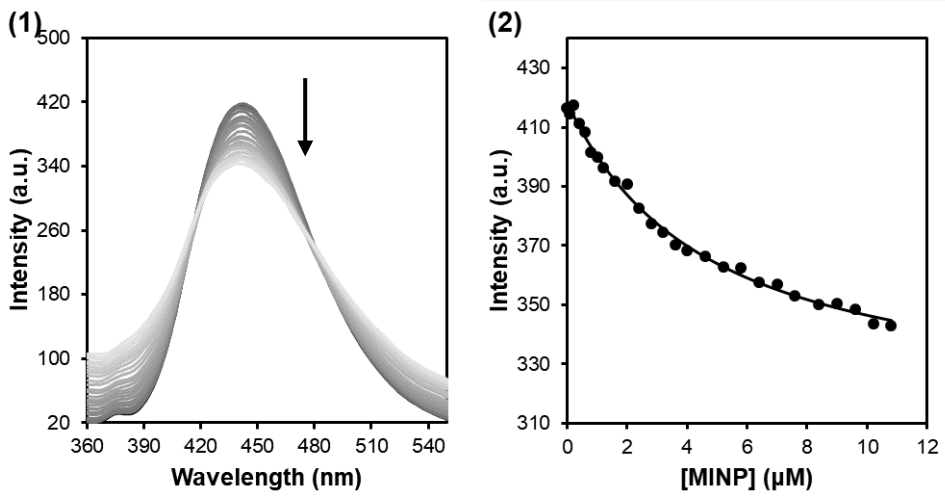

Figure S19. (1) Emission spectra of **6** upon the addition of different concentrations of $MINP_{10}$-CHO in DMF. [**6**] = 0.5 μM. The concentration of MINP was calculated based on an approximate M.W. of 50000 g/mol. λ_{ex} = 338 nm. (2) Plot of intensity at 440 nm with concentration of MINP and nonlinear least squares fitting of the emission intensity at 440 nm to a 1:1 binding isotherm. (Table 1, entry 8)

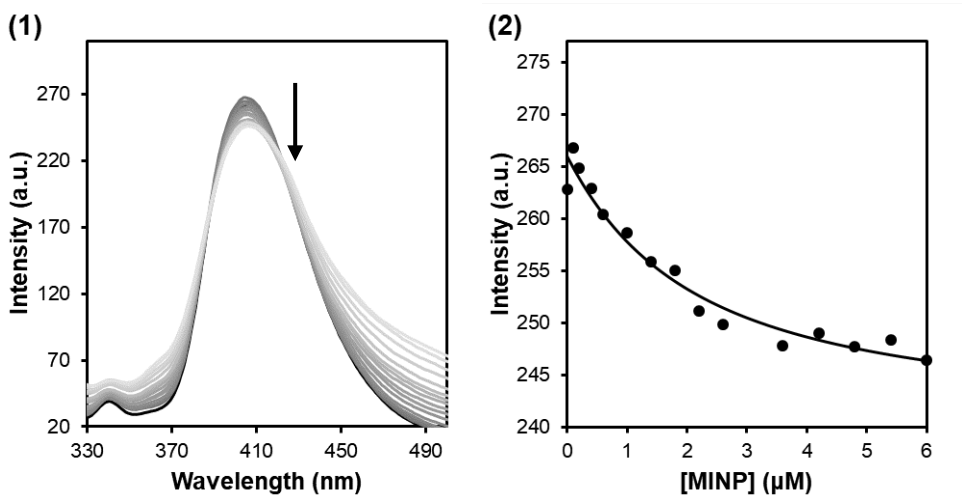

Figure S20. (1) Emission spectra of **9** sodium upon the addition of different concentrations of $MINP_{10}$-CHO in DMF. [**9**] = 0.5 μM. The concentration of MINP was calculated based on an approximate M.W. of 50000 g/mol. λ_{ex} = 309 nm. (2) Plot of fluorescence intensity at 406 nm with concentration of MINP and nonlinear least squares fitting of the emission intensity at 406 nm to a 1:1 binding isotherm. (Table 1, entry 9)

Imine Formation Kinetics.

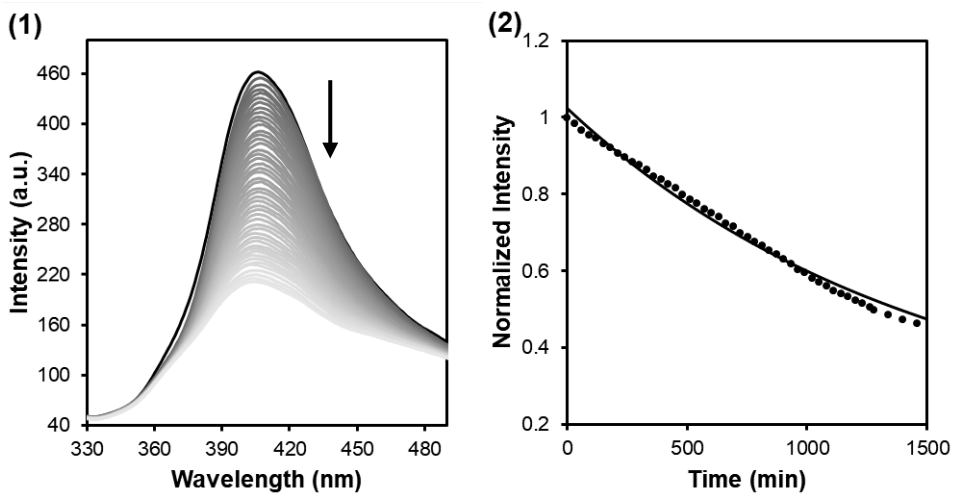

Figure S21. (1) Fluorescence spectra of **5** with 5.0 μM MINP$_4$-CHO with time in DMF at room temperature. [**5**] = 0.5 μM. λ_{ex} = 295 nm. (2) Plot of emission intensity at 406 nm of spectra in (1) and non-linear curving fitting to the first-order kinetics (Table 2, entry 1).

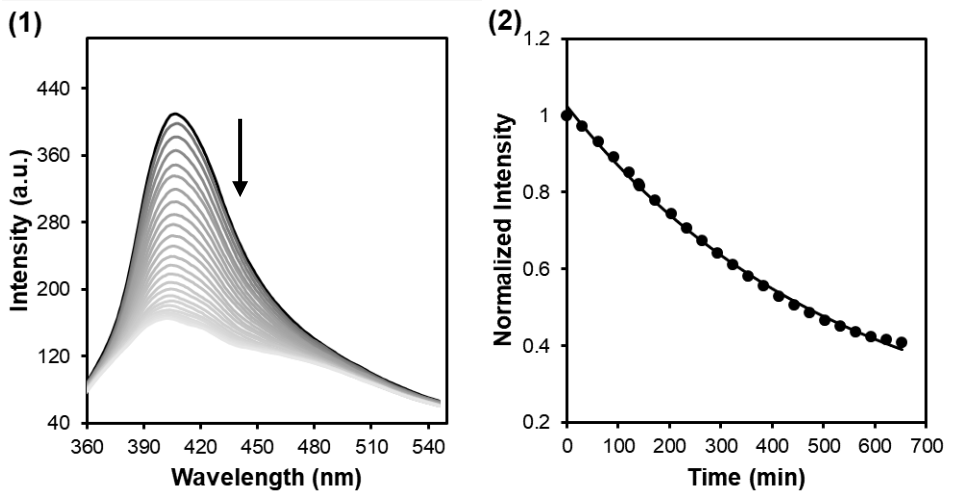

Figure S22. (1) Fluorescence spectra of **5** with 5.0 μM MINP$_4$-CHO with time in DMF at 33 °C. [**5**] = 0.5 μM. λ_{ex} = 295 nm. (2) Plot of emission intensity at 406 nm of spectra in (1) and non-linear curving fitting to the first-order kinetics (Table 2, entry 2).

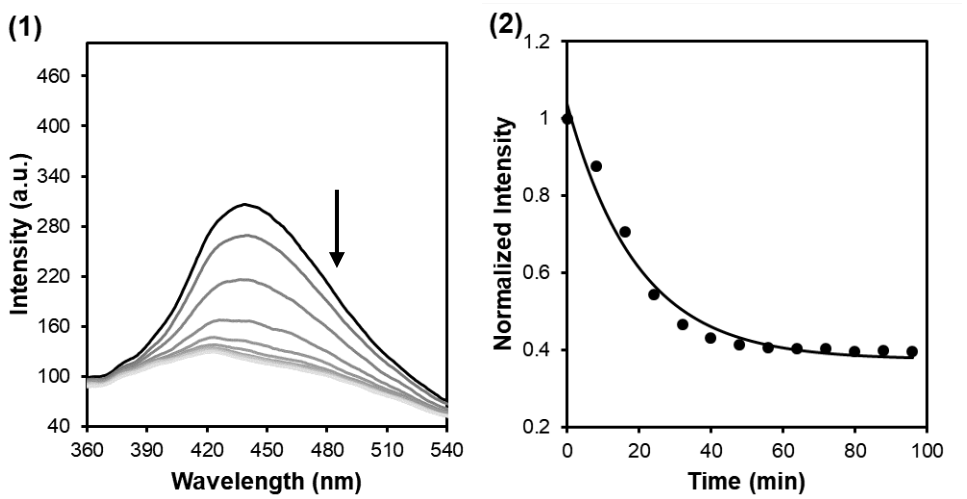

Figure S23. (1) Fluorescence spectra of **6** sodium with 5.0 μM MINP$_4$-CHO with time in DMF at 50 °C. [**6**] = 0.5 μM. λ_{ex} = 338 nm. (2) Plot of emission intensity at 439 nm of spectra in (1) and non-linear curving fitting to the first-order kinetics (Table 2, entry 4).

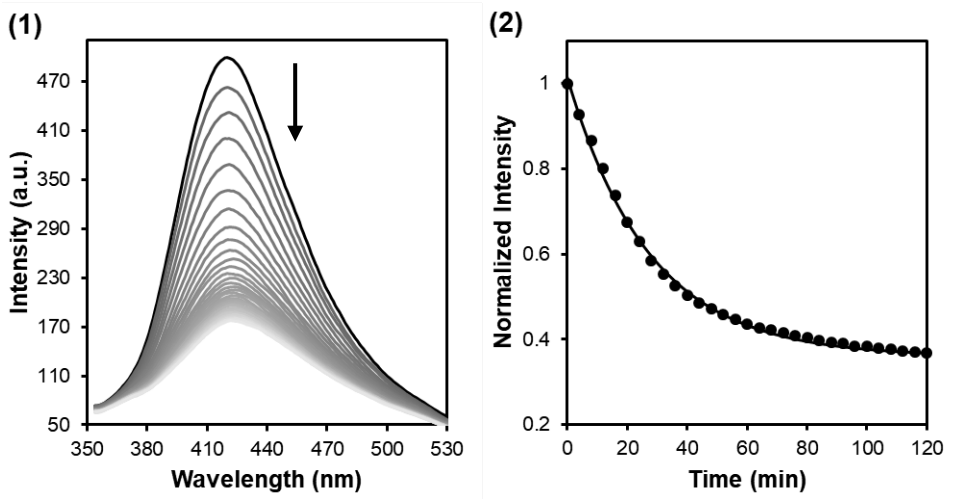

Figure S24. (1) Fluorescence spectra of **7** with 5.0 μM MINP$_4$-CHO with time in DMF at 50 °C. [**7**] = 0.5 μM. λ_{ex} = 335 nm. (2) Plot of emission intensity at 420 nm of spectra in (1) and non-linear curving fitting to the first-order kinetics (Table 2, entry 5).

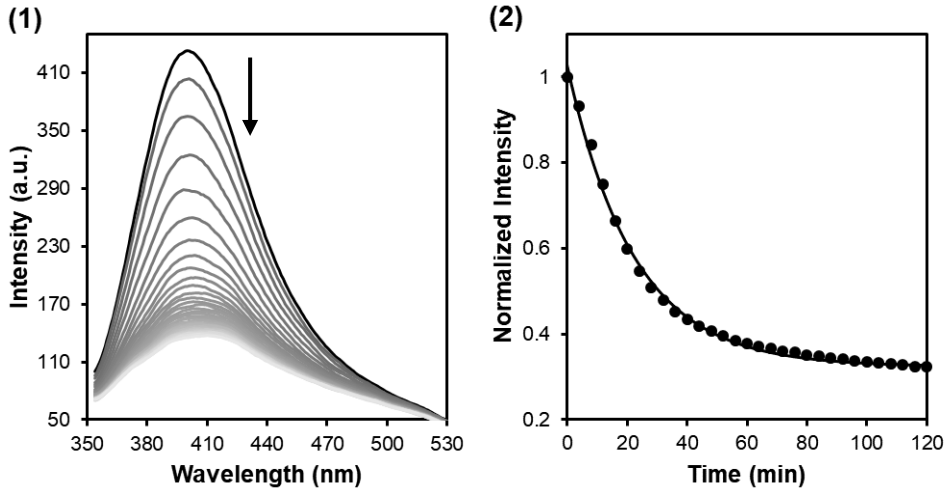

Figure S25. (1) Fluorescence spectra of **8** with 5.0 μM MINP$_4$-CHO with time in DMF at 50 °C. [**8**] = 0.5 μM. λ_{ex} = 335 nm. (2) Plot of emission intensity at 400 nm of spectra in (1) and non-linear curving fitting to the first-order kinetics (Table 2, entry 6).

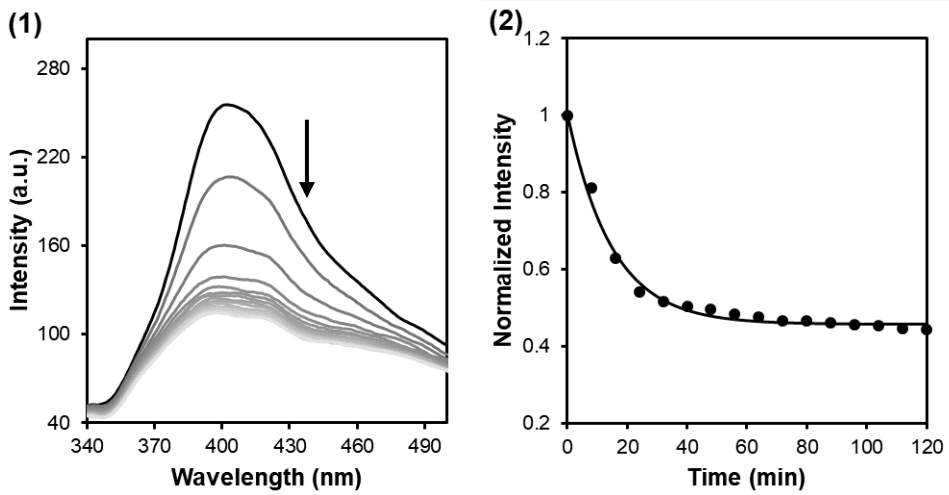

Figure S26. (1) Fluorescence spectra of **9** sodium with 5.0 μM MINP$_4$-CHO with time in DMF at 50 °C. [**9**] = 0.5 μM. λ_{ex} = 309 nm. (2) Plot of emission intensity at 406 nm of spectra in (1) and non-linear curving fitting to the first-order kinetics (Table 2, entry 7).

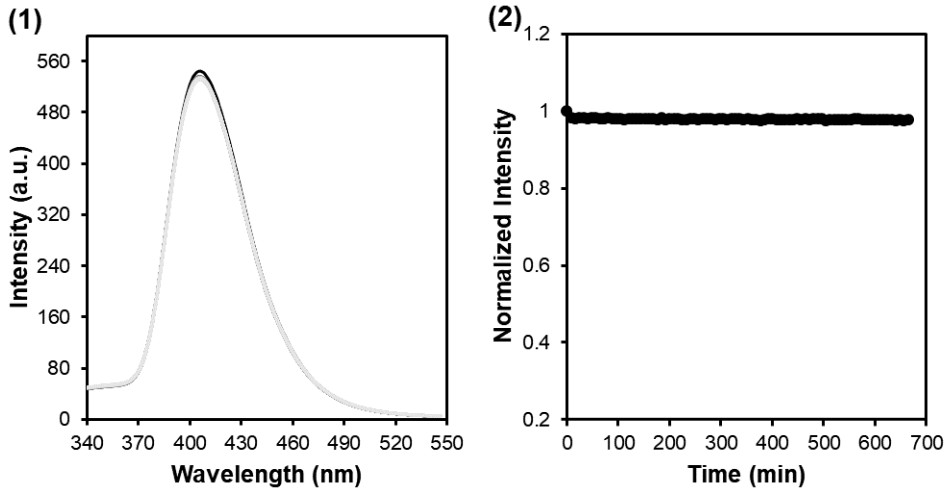

Figure S27. (1) Fluorescence spectra of **5** with 5.0 μM **11** with time in DMF at 50 °C. [**5**] = 0.5 μM. λ_{ex} = 295 nm. (2) Plot of emission intensity at 406 nm of spectra in (1) (Table 2, entry 8).

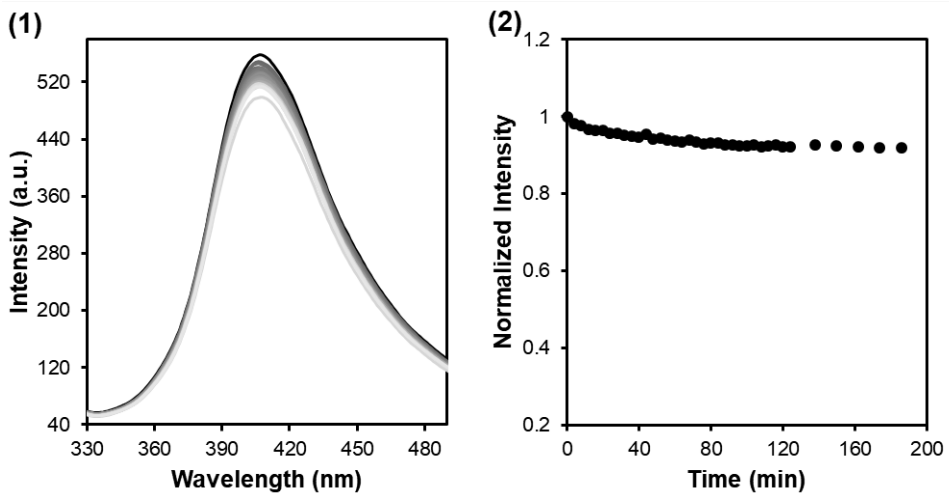

Figure S28. (1) Fluorescence spectra of **5** with 5.0 μM MINP$_4$-CH_2OH (reduced by $NaBH_4$ from MINP$_4$-CHO) with time in DMF at 50 °C. [**5**] = 0.5 μM. λ_{ex} = 295 nm. (2) Plot of emission intensity at 406 nm of spectra in (1) (Table 2, entry 9).

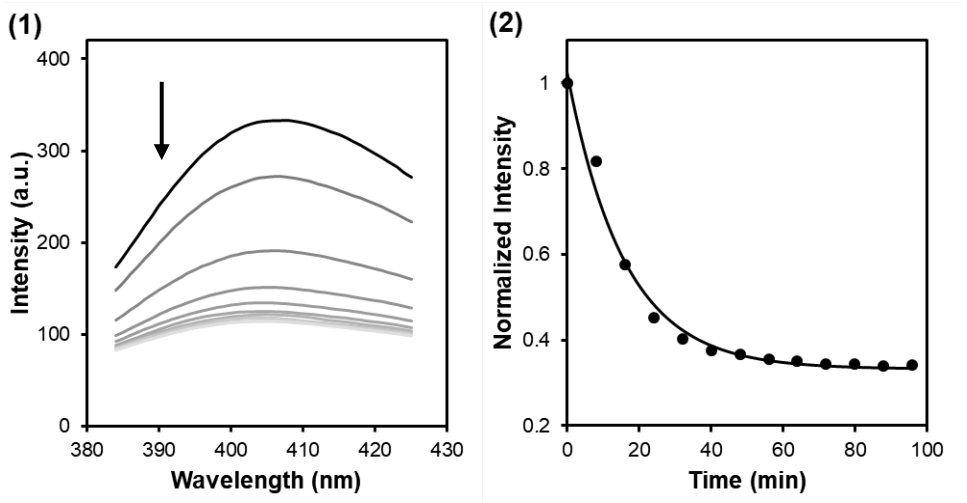

Figure S29. (1) Fluorescence spectra of **5** with 5.0 μM MINP$_{10}$-CHO with time in DMF at 50 °C. [**5**] = 0.5 μM. λ_{ex} = 295 nm. (2) Plot of emission intensity at 406 nm of spectra in (1) and non-linear curving fitting to the first-order kinetics (Table 2, entry 10).

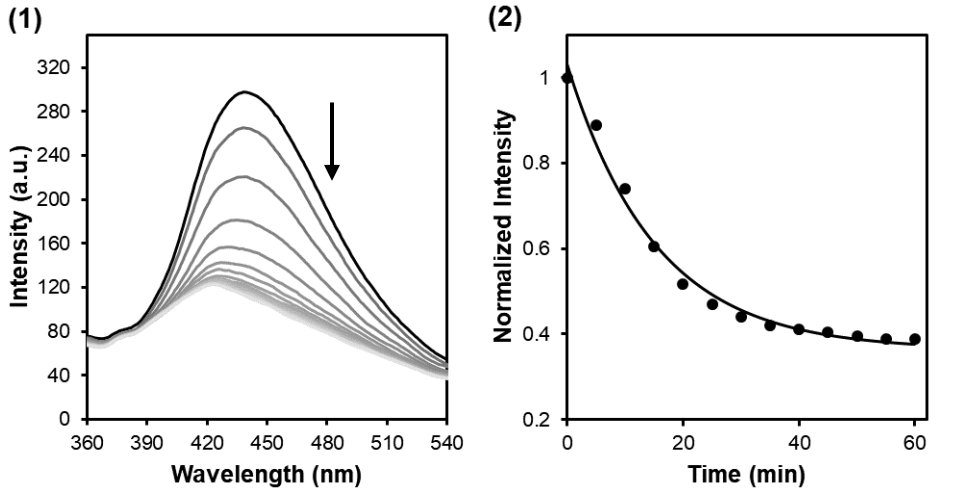

Figure S30. (1) Fluorescence spectra of **6** with 5.0 μM MINP$_{10}$-CHO with time in DMF at 50 °C. [**6**] = 0.5 μM. λ_{ex} = 338 nm. (2) Plot of emission intensity at 439 nm of spectra in (1) and non-linear curving fitting to the first-order kinetics (Table 2, entry 11).

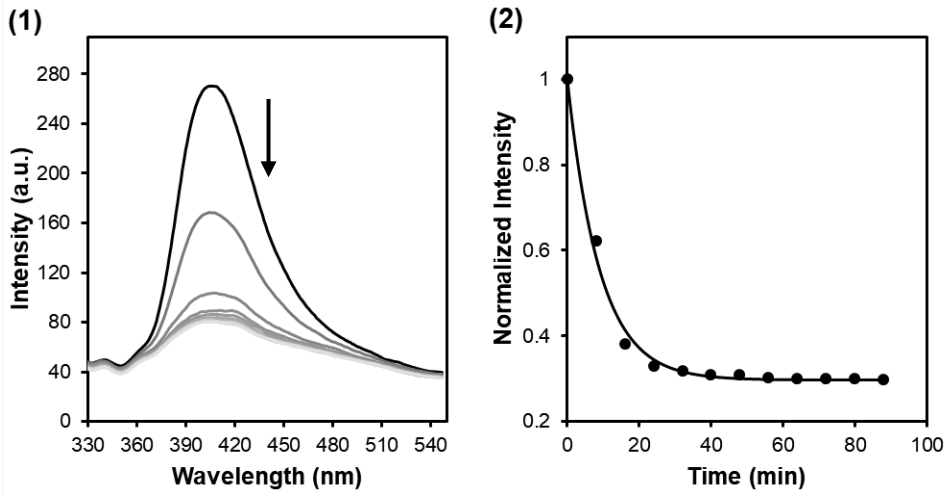

Figure S31. (1) Fluorescence spectra of **9** with 5.0 μM MINP$_{10}$-CHO with time in DMF at 50 °C. [**9**] = 0.5 μM. λ_{ex} = 309 nm. (2) Plot of emission intensity at 406 n°°°m of spectra in (1) and non-linear curving fitting to the first-order kinetics (Table 2, entry 12).

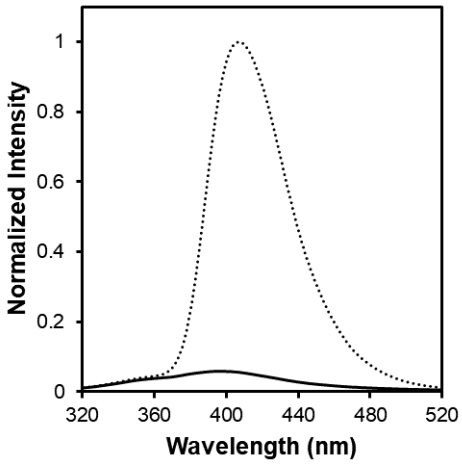

Figure S32. Fluorescence spectra of **5** (dotted line, peak at 407 nm) and **4** (solid line, peak at 396 nm). Normalized at maximum intensity of spectrum of **5**. λ_{ex} = 295 nm. [**5**] = [**4**] = 5.0 μM.

^{1}H and ^{13}C NMR Spectra

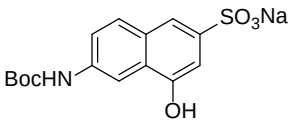

13

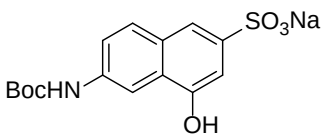

13

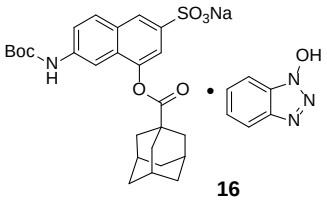
SO3Na
Boc
N
H
O
O
OH
N
N
N

16

10.0 9.5 9.0 8.5 8.0 7.5 7.0 6.5 6.0 5.5 5.0 4.5 4.0 3.5 3.0 2.5 2.0 1.5 1.0 0.5 0.0
f1 (ppm)

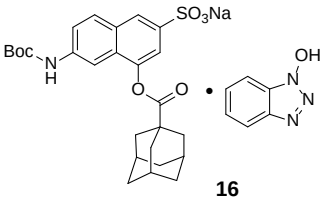
SO3Na
Boc
N
H
O
O
OH
N
N
N

16

200 190 180 170 160 150 140 130 120 110 100 90 80 70 60 50 40 30 20 10 0 -10
f1 (ppm)

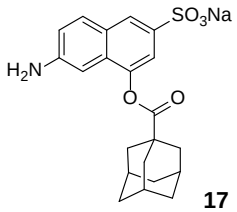
SO3Na
H2N
O
O

17

10.0 9.5 9.0 8.5 8.0 7.5 7.0 6.5 6.0 5.5 5.0 4.5 4.0 3.5 3.0 2.5 2.0 1.5 1.0 0.5 0.0 -0.5 -1.0
f1 (ppm)

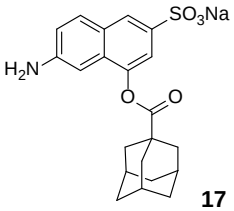
SO3Na
H2N
O
O

17

200 190 180 170 160 150 140 130 120 110 100 90 80 70 60 50 40 30 20 10 0 -10
f1 (ppm)

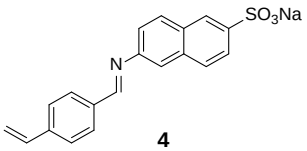

4

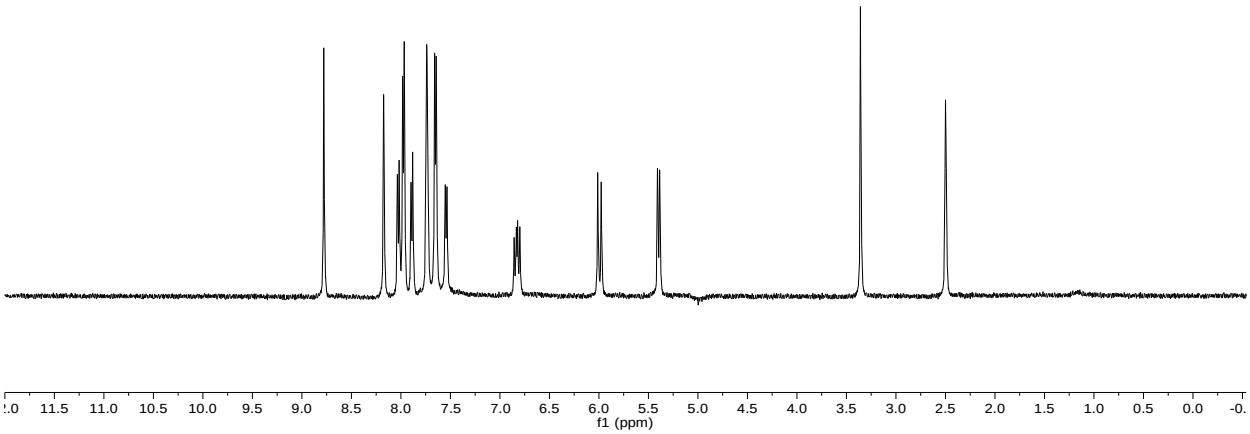

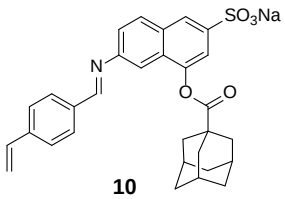

10